

Document Version

Final published version

Licence

Dutch Copyright Act (Article 25fa)

Citation (APA)

Uludağ, M. Ş., & Speretta, S. (2025). Delfi-PQ: In-Orbit Performance and Lessons Learned in Developing a 3P PocketQube. In *Proceedings of the 76th International Astronautical Congress: Sydney, Australia 29 September - 3 October 2025* (1 ed., pp. 609-623). Article IAC-25-B4-6B-6-x100349 (Proceedings of the International Astronautical Congress, IAC). International Astronautical Federation, IAF. <https://doi.org/10.52202/083084-0062>

Important note

To cite this publication, please use the final published version (if applicable).
Please check the document version above.

Copyright

In case the licence states “Dutch Copyright Act (Article 25fa)”, this publication was made available Green Open Access via the TU Delft Institutional Repository pursuant to Dutch Copyright Act (Article 25fa, the Taverne amendment). This provision does not affect copyright ownership.
Unless copyright is transferred by contract or statute, it remains with the copyright holder.

Sharing and reuse

Other than for strictly personal use, it is not permitted to download, forward or distribute the text or part of it, without the consent of the author(s) and/or copyright holder(s), unless the work is under an open content license such as Creative Commons.

Takedown policy

Please contact us and provide details if you believe this document breaches copyrights.
We will remove access to the work immediately and investigate your claim.

IAC-25-B4-6B-6-x100349

Delfi-PQ: In-Orbit Performance and Lessons Learned in Developing a 3P PocketQube

Mehmet Sevket Uludag^{1a,*}, Stefano Speretta^{1b}

^a Department of Space Engineering, Faculty of Aerospace Engineering, Delft University of Technology, Kluyverweg 1, 2629 HS, Delft, The Netherlands

* Corresponding author

Abstract

Delfi-PQ is a pioneering 3P PocketQube developed at Delft University of Technology, measuring 50x50x178 mm and weighing 545 g. Launched on January 13th 2022, it remained operational until its deorbit in January 2024, demonstrating nearly two years of sustained in-orbit functionality. Its architecture features a standardized core that supports reusable hardware and software across multiple subsystems, while an innovative structural design maximizes the limited internal volume. This paper presents results in orbit, the lesson learnt and a detailed hardware development cost analysis of a 3P PocketQube.

Cost containment was a central mission objective. Using commercial off-the-shelf components, modular subsystem design, and iterative manufacturing, the Delfi-PQ team maintained tight budget control. Multiple hardware revisions allowed lessons learnt at each stage to be quickly integrated back into the design cycle. A detailed cost breakdown shows that a standardized core can substantially reduce non-recurring engineering expenses, making advanced pico-satellite development feasible within academic constraints. During its mission, Delfi-PQ encountered substantial thermal swings (up to 75°C), yet consistently maintained full functionality. Although some limitations in battery protection arose from specific design choices, the paper documents which components performed reliably in space and how others deteriorated over time, offering critical guidance for future teams. In addition, the inclusion of a laser reflector payload designed to enhance tracking accuracy and the structural innovations required to optimize space usage are discussed.

A global network of amateur radio operators, together with the ground station in Delft, regularly received telemetry throughout the mission. This support was vital for tracking spacecraft health, investigating anomalies, and refining subsystem performance: the extended reliability of Delfi-PQ underscores the value of cost-conscious engineering, modular architectures, and strategic community partnerships to extend the service life of the mission. In summary, Delfi-PQ demonstrates that a lean yet robust satellite design based on modular principles, iterative development, and close collaboration can reliably operate over extended mission durations. By presenting a full cost breakdown and comprehensive mission results, this paper offers practical insights for institutions aiming to deploy similarly innovative, affordable PocketQubes for advanced research and education.

1. Introduction

Over the past two decades, there has been a large increase in satellite launches, primarily driven by the emergence of small satellites, sometimes as small as a few hundred grammes. This trend started from universities, where the budget is somewhat limited, but later also extended to commercial entities, capable of finally shortening the development cycle compared to previous missions [1]. This paper focuses on the Delfi-PQ mission, a cubic-shaped satellite comparable in size to a 0.5 l water bottle, developed by the Delft University of Technology [2, 3].

The satellite is composed of smaller units, with a size

of 50x50x50 mm with a maximum mass of 250 g, called PocketQubes (PQs) [4]: Delfi-PQ is composed of 3 such units (also called Ps) and it can be seen in Figure 1. The limited size of such satellites inherently constrains the size of subsystems and payloads, prompting a shift in mission concepts towards creating simpler missions. Due to their compactness and relatively low development costs, they can be launched as large formations to form distributed sensor networks, further reducing overall mission cost. The primary goal of Delfi-PQ is to establish the foundation for a series of very small satellites developed at Delft, where students and researchers can play a key role in the mission.



Fig. 1: The Delfi-PQ flight model.

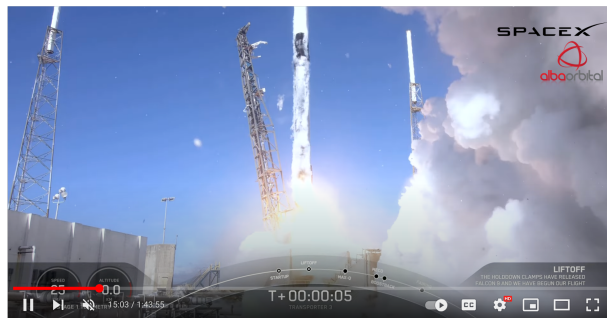


Fig. 2: The Delfi-PQ launch on Jan 13th 2022.

This paper briefly introduces the Delfi-PQ mission and focuses on the lesson learnt from 2 years in-orbit operations, until its natural decay on January 6th 2024, providing an important example for teams that are working on similar missions. An analysis of the satellite systems is presented to conduct the reader through the problems encountered and the solutions that have been employed to carry out the mission. The paper then continues by analyzing the mission cost and presenting the solutions the team implemented to maintain the mission development cost low and still achieve the mission objectives [5].

2. Design Approach

2.1 Modularity

The first design choice that was made on the system was to boost modularity by separating all key functionalities in the satellite in separate boards and making sure they

could be connected by a lean interface. The separation of concerns in different boards, with minimal to no interaction made each subsystem more complex but allowed a clear separation of concerns, ultimately simplifying the high-level design.

Great efforts were spent on the definition of a lean shared bus [6] for very small satellites, based on a minimal set of functionalities and providing a reduced footprint on each board. This included data communication, power transmission, and an emergency reset mechanism that could be used by any subsystem detecting anomalies to request a general satellite power cycle.

To further simplify the design, a single-string satellite architecture was enforced to simplify the design, assuming that redundancy would be provided at mission level by employing multiple satellites for the same mission. This is in line with the general trend for small satellites [1], trying to leverage the economies of scale, which emerges when building multiple identical satellites, to lower the overall cost of mission. Simpler systems often require simpler testing strategies and thus can benefit from better coverage (with respect to similar missions) and thus higher reliability.

2.2 Defining a Core

The modularity choice, taken very early in the design, led the team to assign basic satellite functionalities to independent systems interconnected by a shared bus. This required similar components to be used on each system, ultimately leading to the design of a “core” electronic suite, comprising key functionalities. This included the capabilities of communicating on a digital bus, monitoring of current consumption, a re-triggerable current limiter, a watchdog and a Micro Controller Unit (MCU). This basic building block has been designed very early in the mission timeline and has been extensively tested to guarantee its functionality and its tolerance to eventual failures in space. Then it has been introduced into all satellite subsystems designs: this also led to a general cost reduction thanks to a general simplification of the different subsystem designs.

The core logic ultimately included multiple functionalities, as shown in Figure 3, including:

- **Protection circuit** used to monitor the system current consumption and limit the maximum current consumption in the event of faults. A persistent fault leads to the subsystem power-cycling to attempt to solve the problem, if temporary. More details on this system can be found in Section 2.3.2.
- **MCU** providing monitoring and control of the sub-

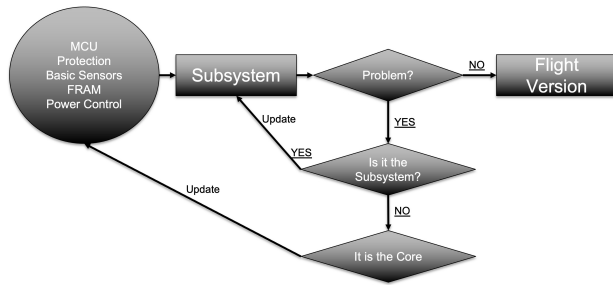


Fig. 5: Iterative subsystem development cycle.

grated together, leading to multiple test sessions involving a large part of the satellite. This allowed us to move relatively quickly and extensively test the satellite parts, limiting the final integration and testing process: the team became very skilled in the satellite integration, having practiced it multiple times, to the point that the final flight model integration could be carried out within one afternoon.

2.3.2 Protection Circuit

Given the reliance on Commercial Off-The-Shelf (COTS) devices, the design mitigates radiation-induced single-event latch-ups (SEL). We adopted a two-tier strategy: (i) critical rails use a re-triggerable electronic current limiter sized to bound worst-case dissipation and enforce a sufficient off-time to extinguish the latch; (ii) lower-risk Integrated Circuits (ICs) include series limiters dimensioned to preserve nominal operation while capping transient power. Because per-IC breakers would be area-prohibitive, groups of ICs share one limiter, while each device retains its own series resistor. Board MCUs monitor functionality and can request a subsystem or full-spacecraft power cycle if a “soft” latch disrupts operation without a large current rise. This scheme proved effective in orbit: telemetry shows multiple autonomous trip-and-recover events with no lasting degradation.

2.4 Software

To match the hardware core, embedded software was architected for reuse. A single MCU family was used across boards; common low-level libraries and a thin RTOS layer (based on FreeRTOS) were shared. Test apps followed a hierarchical structure so the same procedures could validate multiple boards. In-flight update capability was designed into all subsystems: MCU flash was partitioned into one write-protected golden image (programmed pre-launch) and two update slots. Boot failures or runtime health checks trigger a rollback to the golden image. This

strategy shortened the on-ground development cycle by safely deferring advanced functions to post-launch updates.

2.5 Satellite Bus

The spacecraft comprises the Electrical Power System (EPS) with battery board and solar panels, Communication System (COMMS) (main transceiver, power amplifier daughter board, and antenna phasing board), On-Board Computer (OBC), a secondary OBC for on-orbit experimentation, the Antenna Deployment Board (ADB), and the Attitude Determination and Control System (ADCS) with three-axis magnetorquers [11]. High-level block diagrams are shown with the subsystem descriptions below.

Electrical Power System (EPS). The EPS comprises the main board, battery board, and solar panels. Building on the core (Fig. 3), Fig. 6 shows the inhibit switches and four unregulated buses; each bus is protected by a current-limited power switch. BUS-1 (powering COMMS and OBC) is normally ON, while others are enabled only as needed. The bus voltage spans 3.0–4.2 V and allows up to ~4.5 W continuous load. Each solar cell is paired with its own MPPT for efficient generation [12].

The battery board integrates two 750 mAh Li-ion cells, a protection circuit, inhibit switches, and spring-loaded connectors for the solar panels (Fig. 10). To comply with launcher requirements, the inhibit switches disconnect the battery return line. The protection logic halts discharge below 2.8 V, stops charge above 4.2 V, and disables the cells outside the 0–40°C range. A side effect of the bypass-diode drop across the charge FET during temperature protection is the risk of EPS brownouts during high-current transients (e.g., COMMS TX). The self-discharge behavior of the protection circuitry was also characterized by enabling both inhibit switches and monitoring cell voltages over time (Fig. 9) [13].

Panels on $\pm X$ and $\pm Y$ sides host two cells each, with MPPTs and power/temperature telemetry. In orbit, panel temperatures varied between -40°C and $+40^{\circ}\text{C}$.

The EPS main board went through four revisions (final: electronics 456 €, PCB 213 €), the battery board four (final: 386 € electronics, 221 € PCB), and the four-panel set three (final: 308 € electronics, 1061 € PCB). Twenty solar cells were procured for 7000 €, eight of which were integrated. Costs assume lots of five.

On-Board Computer (OBC). The OBC provides commanding, subsystem interfacing, and data handling. Relative to the core (Fig. 3), it adds a microSD card (with level shifting and protection) and a 40-pin daughterboard connector exposing one unregulated bus, an Inter-Integrated

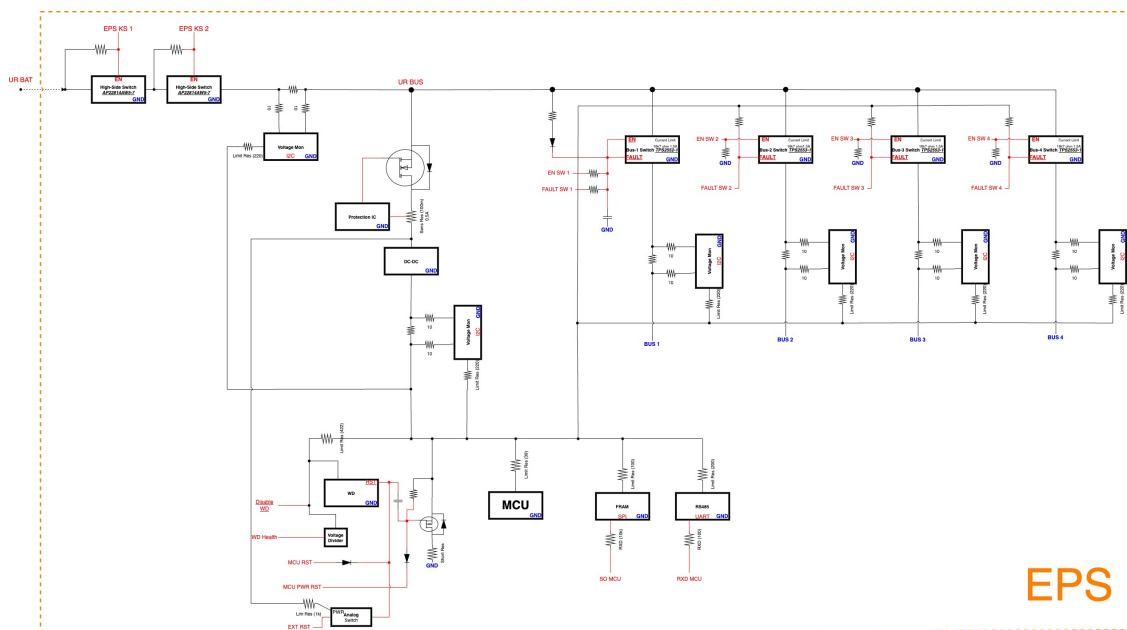


Fig. 6: Electrical Power System (EPS) high-level block diagram.

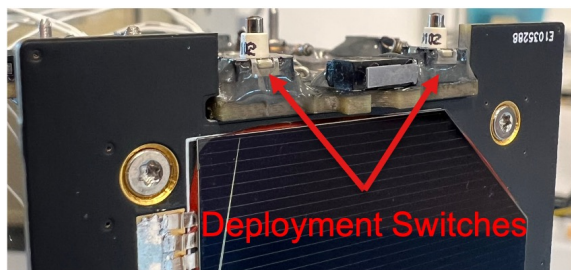


Fig. 7: Deployment/separation switches on the $-Z$ side.

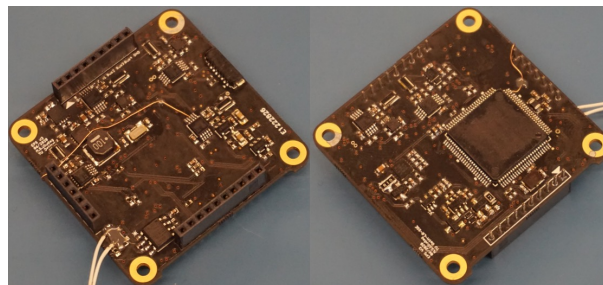


Fig. 8: Electronic Power System board assembly.

Circuit (I2C) line (plus two optional I2C), two optional Serial Peripheral Interface (SPI), and general-purpose I/O. A planned Global Navigation Satellite System (GNSS) payload (later omitted) led to a second OBC being flown as an in-orbit lab. Full in-flight software updates are supported. The OBC had two revisions (final: 388 € electronics, 99 € PCB; ~97 € per unit when amortized over five).

Communication System (COMMS). COMMS comprises [14]: (i) a transceiver board interfacing the bus and handling modulation/demodulation (two Semtech SX1276 plus an MCU for framing/protocol), (ii) an Radio Frequency (RF) amplifier daughterboard with a 1 W PA (Qorvo RFPA0133) supporting stepped power (0.25/0.5/1 W, ~55–65% efficiency) and an LNA for full-duplex sensitivity, and (iii) an antenna phasing board

combining monopoles/dipoles for the uplink/downlink and routing GNSS feeds. The main board had three revisions (final: 384 € electronics, 120 € PCB), the PA daughterboard two (final: 384 € electronics, 90 € PCB), and the phasing board two (final: 252 € electronics, 111 € PCB). Five units of each were produced (~268 € per board when averaged).

Attitude Determination and Control System (ADCS). The ADCS reduces post-deployment tumbling using three air-core magnetorquers and a Bosch BMX055 Inertial Measurement Unit (IMU). Coarse pointing accuracy of ~20° was targeted. Two revisions were produced; the final BOMs were: 474 € electronics, 163 € PCB, 281 € 3D-printed coil formers, and 27 € copper wire (coils man-

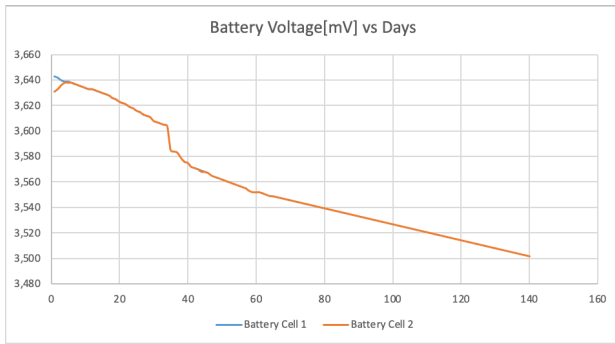


Fig. 9: Cell voltage levels over time under "deployer configuration."

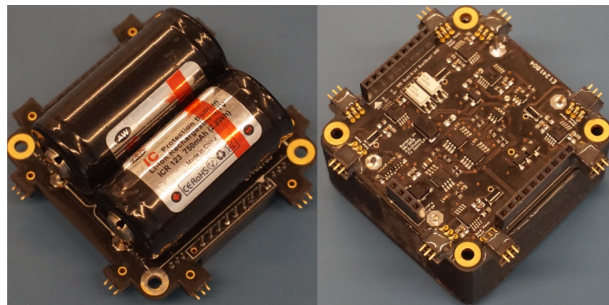


Fig. 10: Battery board with spring-loaded panel connectors.

unfactured once for the flight set). Per-board total ~814 €.

Antenna Deployment Board (ADB). Because the deployed COMMS antennas exceed the stowed envelope, the ADB releases four monopoles using thermal knives, commanded by the OBC nominally 15 minutes after separation. Safety logic enforces battery state/temperature checks and timeouts. Three revisions were made; the final costs were 412 € (electronics), 180 € (PCB), 2500 € (springs), and 2270 € (gold-plated brass monopoles, 3 mm diameter). Lots of five yielded ~1072 € per board.

2.6 Payloads

2.6.1 Low-Frequency Low-Noise Amplifier (LNA)

A technology demonstrator for future low-frequency radio-astronomy missions (500 kHz–1 MHz). Given ionospheric opacity and terrestrial noise, the goal was not scientific observation but survivability and measurement of strong man-made signals. A simple RF channel-power estimator (SX1276) swept the band via a custom up-converter to the receiver band. The antenna path leverages the COMMS phasing assembly (Sec. 2.5).

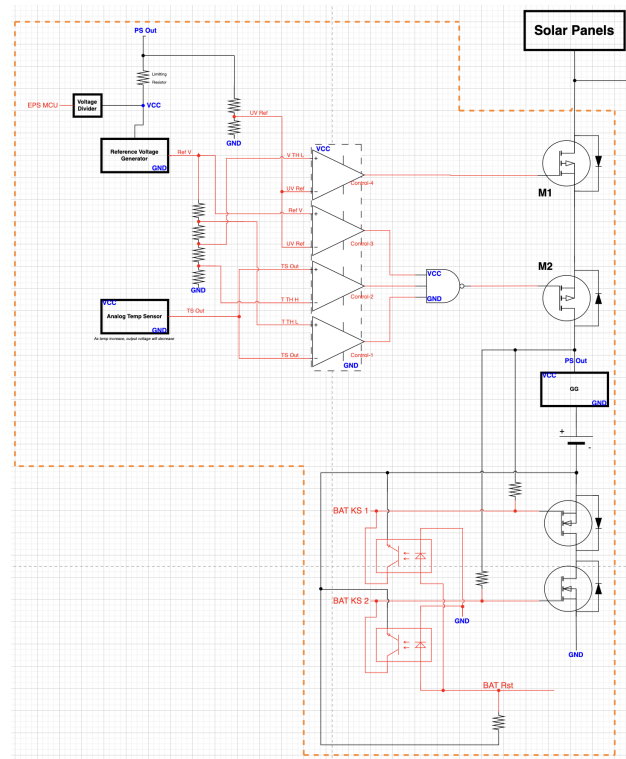


Fig. 11: Battery protection circuit diagram.

2.6.2 Laser Reflectors

Four laser retroreflectors were mounted near the long-face geometric centers to enable satellite laser ranging (SLR) and compare precise SLR orbits against radar-derived ephemerides, informing tracking accuracy for very small spacecraft.

2.6.3 GNSS Receivers

Two differential GNSS receivers were planned, mounted with a fixed baseline to de-risk formation-flying navigation. Pandemic-related delivery delays prevented integration prior to environmental testing, so the receivers were omitted from the flight build.

2.6.4 Secondary OBC (In-Orbit Lab)

Originally a data recorder for the GNSS payload, the second OBC flew without flight software and now serves as a sandbox for student experiments (e.g., telemetry forecasting onboard), safely isolated from the primary command/data path thanks to the in-flight update and rollback scheme described in Sec. 2.4.

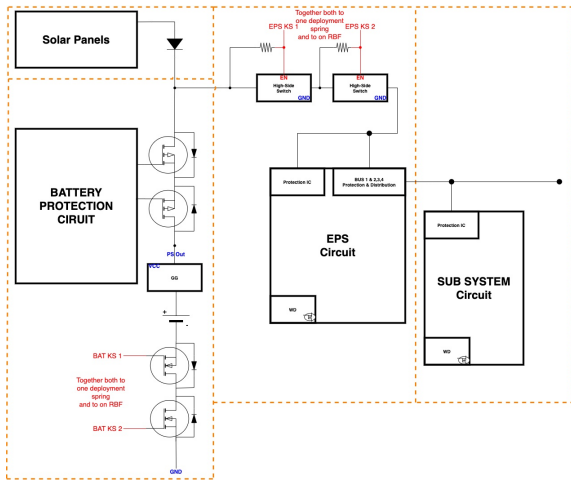


Fig. 12: High-level Electronic Power System protections and inhibit switch concept.

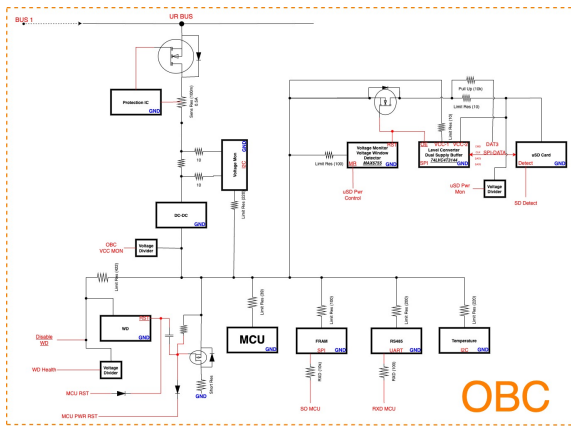


Fig. 13: OBC high-level block diagram.

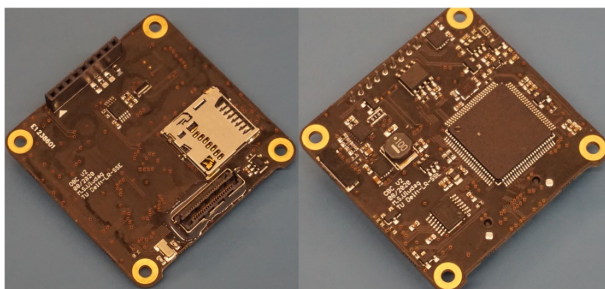


Fig. 14: OBC board assembly (top and bottom).

3. Lessons Learned

The Delfi-PQ project was the first one for the team where an iterative design process was attempted, while all

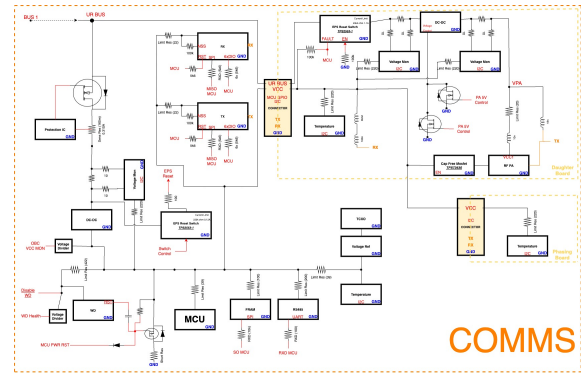


Fig. 15: COMMS high-level block diagram.

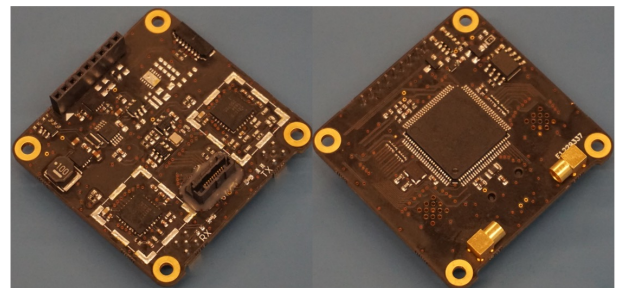


Fig. 16: COMMS transceiver board (top/bottom).

previous missions followed a traditional V-cycle. It was also the first project in Delft employing a PQ as compared to the previous CubeSat missions. There are thus several lessons learned on the mission and this section will focus on them, starting from the early design iterations, the final integration and testing and the in-orbit phase.

3.1 Early design phases

The Delfi-PQ mission was the first attempt in Delft to develop a PQ and it required a large rethink of the devel-

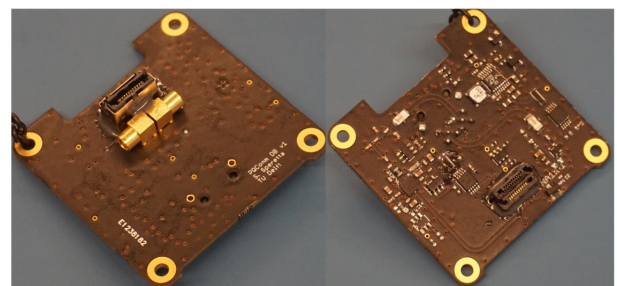


Fig. 17: COMMS RF daughterboard with PA/LNA (top/bottom).

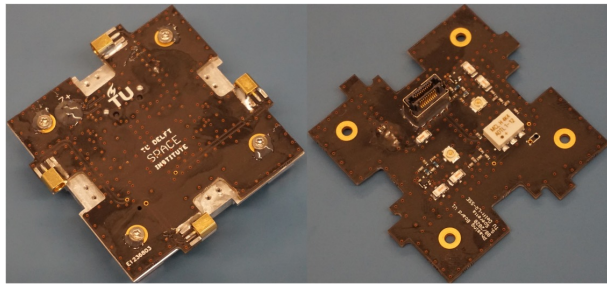


Fig. 18: COMMS antenna phasing board (top/bottom).

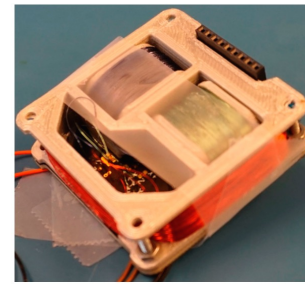


Fig. 21: Three-axis air-core magnetorquer assembly.

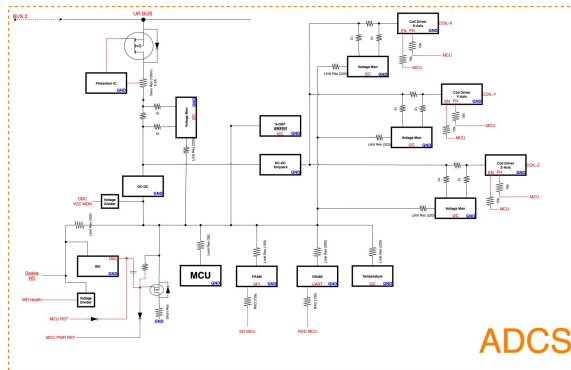


Fig. 19: ADCS high-level block diagram.

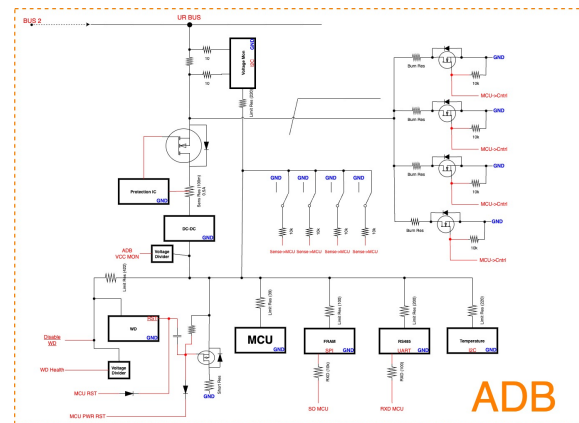


Fig. 22: Antenna Deployment Board (ADB) high-level block diagram.

opment strategy, especially because the available volume is so much more limited with respect to a CubeSat [10]: in particular, connectors and cables occupy a significant volume and constrain the design significantly. This led to a series of attempts to limit as much as possible the interconnections inside the satellite, ultimately leading to the development of a very simple shared bus and forcing all subsystems to be directly connected to it. Some of these attempts are documented in [6], where initial concepts have been proposed.

The iterative development cycle philosophy had also

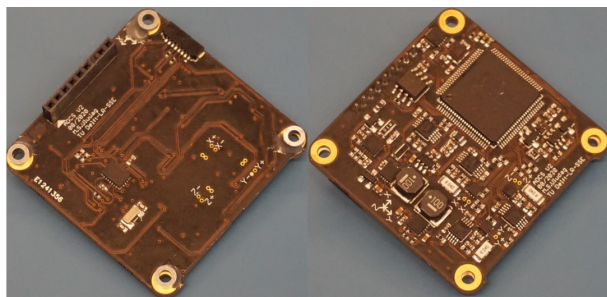


Fig. 20: ADCS board assembly.

been attempted for the first time in Delft and this required the whole team to get used to short sprints, where a minimum viable product would be the output, instead of a fully developed subsystem: this can be clearly seen in the large number of prototypes that were produced, as shown in Figure 26. The availability of parts in the very early stages allowed the team to frequently integrate the satellite, evaluating the consequences of many choices very quickly. Most of these prototypes were only very limited in features, but this helped to get acquainted with the new form factor very clearly. As mentioned above, the relatively large volume taken by connectors and cables became very quickly evident.

Another challenge that became evident very early in the mission was the difficulty in fitting tools during the satellite assembly: the electronics occupied the large majority of the internal volume and very little space was still available. The team started integrating electronic and mechanical design to try and maximise the limited available space, also simplifying the satellite structure and using electronic boards as structural elements, especially for the

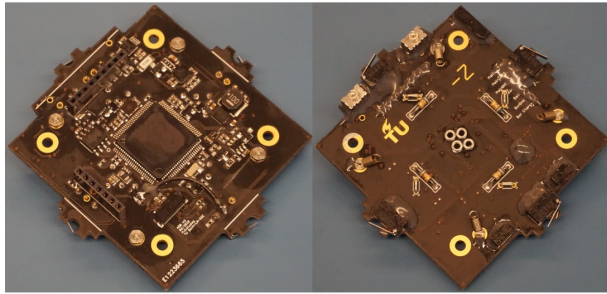


Fig. 23: ADB board assembly.

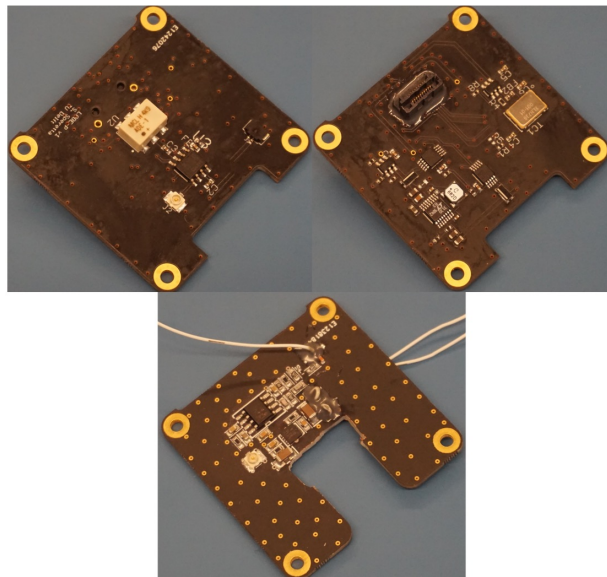


Fig. 24: LNA mixer board (top) and LNA front-end (bottom).

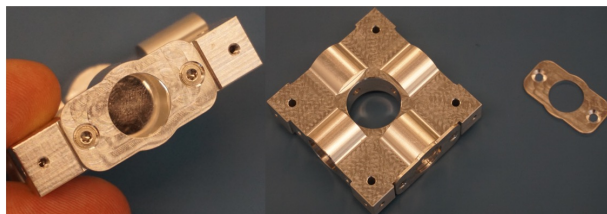


Fig. 25: Laser reflector, holder, and cover.

solar panels.

One creative solution adopted by the team has been the use of spring-loaded connectors to replace cabling to the solar panels: these connections were established electrically only once the panels had been placed in position and the screws tightened. This solution allowed to avoid



Fig. 26: An overview of all the components developed for the Delfi-PQ mission.

the space consumed by the folded cable and the connectors while still providing a reliable connection to simple contact pads. After an initial vibration test, it was determined that the scratching caused by the contacts on the pads was barely noticeable, as shown in Figure 27. Alignment of such contacts proved challenging, due to the very small separation, but this could be solved with alignment pins that prevent short circuits when the panels are not correctly aligned.



Fig. 27: Spring-loaded contact pads after vibration testing, showing no visible sign of wear.

To mitigate radiation effects, particularly single-event latch-ups, we implemented a board-level protection circuit providing over-voltage, under-voltage, and over-current trip functions. A fully discrete realization would have exceeded the available board area on each subsystem, so we evaluated COTS protection ICs. Most available de-

vices target higher-power rails, whereas our steady-state loads were typically $< 15\text{ mA}$ at 3.3 V. For area and efficiency reasons we also selected COTS DC–DC converters, which introduced a secondary effect: start-up inrush currents on the order of 100 mA triggered nuisance over-current trips during subsystem boot. The final configuration balanced latch-up immunity with start-up transients; on-orbit telemetry shows multiple autonomous trip-and-recover events without lasting degradation, indicating the protection scheme prevented fault propagation and contributed to overall availability.

3.2 Satellite integration and testing

Satellite integration has been extremely challenging as it occurred during a lock-down period due to COVID pandemic in 2020: due to the specific regulations in The Netherlands, all students in the university have been sent home and only a limited number of staff members was allowed in campus: this forced the team to work mostly from home while only two or three team members were integrating the hardware, often in video conference with the rest of the team. This period was also very challenging for the delivery of components that experienced significant delays: this was the case for the satellite GNSS receiver that, unfortunately, had been delivered only few days before the environmental testing campaign and could unfortunately not be integrated. Testing facilities have also been mostly unavailable due to restricted travel protocols, pushing the team to find creative solutions.

Unfortunately, the environmental testing campaign had to be shortened and the thermal equilibrium tests had to be skipped due to the limited availability of personnel to run the test, and this resulted in critical problems during operations (more details in the next section). Full temperature cycling was carried out on the satellite and this allowed to uncover a critical problem with the antenna deployment system not being able to release the on-board receiver antenna at low temperatures. The problem was caused by a combination of an increased battery impedance and underestimated connector resistance, which led to the thermal knife not being able to melt the restraint wires. The replacement of the connection wires allowed to successfully demonstrate the antenna deployment, as shown in Figure 28.

The vibration test also provided an interesting lesson learnt: as the satellite structure was composed of fewer load-bearing elements and many more PCBs with components and spring-loaded connections, changes were easily noticeable in the sine sweep results shown in Figure 29. After carefully inspecting the satellite and repeating the

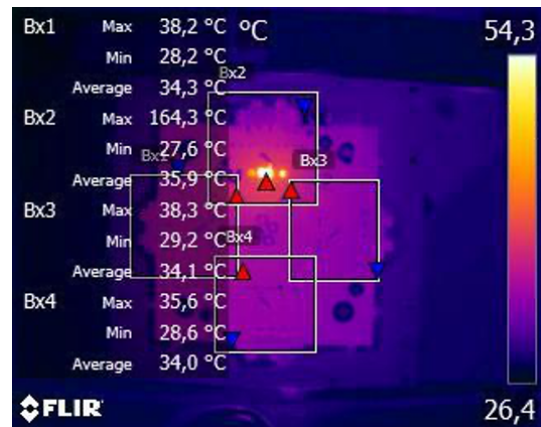


Fig. 28: Infrared image during a knife-heating deployment test [15].

tests, it was demonstrated that the structure was not fully rigid. After careful analysis, it was possible to demonstrate that the frequency shift was associated with modes with an effective mass less than 10% of the satellite (as specified in ECSS-E-ST-10-03C).

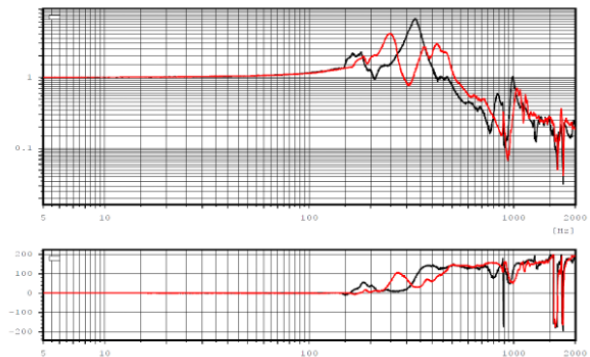


Fig. 29: Sine sweep test result showing the changes before (black) and after (red) random vibrations.

3.3 Operations

As mentioned previously, one critical test had to be skipped during the final environmental campaign, the thermal balance test. Unfortunately, this had severe consequences on the mission as it would have revealed that the thermal equilibrium point was much lower than expected, and close to approximately 0°C. This caused the battery to operate at a temperature lower than expected and, thus limiting the peak current that could be delivered. A battery

heater was initially considered for the mission but due to the very low power available and the thermal simulations (which could not be validated by test, unfortunately), it was removed.

The satellite battery, using Li-Ion chemistry, operated in orbit between -10°C and $+10^{\circ}\text{C}$ but, delivered a very limited current at temperatures below 0°C : due to the final satellite orbit (Sun-synchronous with an altitude of 525 km and an longitude of the ascending node (LTAN) of 10:30), the satellite was in its coldest orbital point over The Netherlands during the winter (as the North pole was not illuminated). Unfortunately, this was the period when students were most available for operations, meaning that the controllability of the spacecraft was very limited. The satellite was operating nominally during the summer but the operations team had a very limited availability. This problem was caused by the battery having a very limited output current at low temperatures together with the large current consumption from the satellite radio, causing the battery to dip below its minimum voltage during transmissions and thus causing the satellite to enter safe mode.

As the battery could experience temperatures below 0°C and this could cause damages during charge, it was decided to implement a system that could selectively stop the charging process at low temperatures (Figure 11). Due to the circuit configuration, an additional voltage drop of approximately 0.4 V was present across the protection switch at the time of launch, but, due to the accumulated radiation dose in space, this rose to 0.9 V at the end of the mission. This additional voltage drop was present only when the battery was below 0°C and this turned out to be the case for most of the satellite passes over The Netherlands (excluding the summer ones). This made sure the battery would appear less charged than it actually was and thus it causing the protection system to trigger more often, making the mission difficult to control. Considering the added complexity introduced by the current protection circuit and its fragility during operations, a different battery system should be considered for future systems. The addition of a heater would prevent many of the problems, but it would also impact the satellite power budget. For this reason, a different battery technology would be advised to cope with the low temperatures.

4. Hardware Development Cost

4.1 Scope and Accounting Approach

All monetary figures in this section are reported in euros and include the Netherlands' Value Added Tax (VAT) (21%), unless noted otherwise. The scope is limited to *hardware development* for the flight article and associated

engineering builds procured during 2017–2020; it excludes personnel, facilities, launch, and operations. Procurement was executed in small batches (typically five boards per run) to de-risk manufacturing, support parallel testing, and seed a spare pool. Because multiple design iterations were intentionally flown through the development pipeline, the totals reflect the true cost of maturing the hardware, not merely the bill of materials for a single, finalized set.

4.2 Aggregate Cost Breakdown

The total hardware outlay over the development period was approximately 86.6 k€. Figure 31 shows how this spend distributes across four accounting buckets that we used for internal budget tracking:

- **Electronics** (components, assembly consumables): ~44.0 k€ ($\approx 50.8\%$).
- **PCB fabrication** (boards, stencils): ~11.6 k€ ($\approx 13.4\%$).
- **Mechanical** (structure, antennas, fasteners, custom parts): ~23.4 k€ ($\approx 27.0\%$).
- **Support** (test jigs, harnessing, generic bench hardware): ~7.1 k€ ($\approx 8.2\%$).

Percentages are computed relative to the total and may not sum exactly to 100% due to rounding and minor allocation residuals. Two practical heuristics emerge for early-phase budgeting: (i) electronics + PCBs together consumed roughly two-thirds of the hardware budget, and (ii) mechanicals were a solid quarter, reflecting both the structural stack and RF/antenna hardware that tend to be cost-dense in small runs.

4.3 Time-Phased Expenditure

Figure 30 summarizes the spend profile as the design matured:

- **2017** (concept-to-EM ramp): the initial spike corresponds to standing up the core electronics and first EMs; eight production runs were executed.
- **2018** (system bring-up): cumulative spend reached ~43 k€ by year end as most subsystems reached first stable revisions; eleven runs were executed.
- **2019** (remote test infrastructure & hold): 10 k€ for the year (~53.75 k€ cumulative) while office access constraints shifted investment toward support equipment and flatsat setups; five runs were executed.

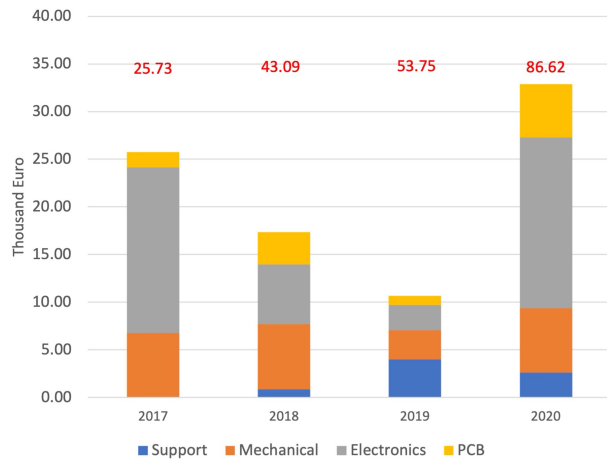


Fig. 30: Cost per year of Delfi-PQ. Numbers in RED are the cumulative cost of the satellite throughout the years [5].

- **2020** (flight maturation & delivery): ~32.9 k€ for the year (total ~86.6 k€), driven by final PCB spins and component buys for the flight build; fifteen runs were executed.

This temporal pattern is typical for educational or first-of-a-kind small missions: an upfront surge to establish the architecture and tooling, a plateau while integration and test stabilize, and a final step during flight-qualification spins.

4.4 Revision Economics and Batch Strategy

Two choices had outsized impact on cost containment:

1. **Standardized subsystem core.** A common core (MCU, DC-DC, telemetry/protection, RS-485, watchdog, FRAM) reduced non-recurring engineering per board and shortened debug loops. As a result, incremental spins targeted only the value-adding circuitry, containing both PCB area and component diversity.
2. **Batch-of-five builds.** Ordering in lots of five balanced price breaks against inventory risk, enabling one flight-representative unit, one engineering model, and spares for destructive tests and regression. For small teams, this batch size also smooths lead-time variability without over-capitalizing on stock.

Across 2017–2020, we executed 39 manufacturing runs (8 + 11 + 5 + 15). While each spin incurs fabrication and assembly overhead, the cumulative effect is lower program

risk and fewer late re-spins near delivery—ultimately protecting the schedule and the total cost.

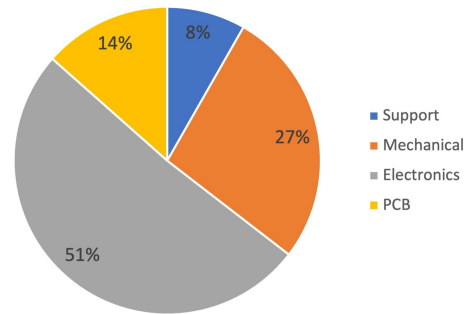


Fig. 31: Cost Breakdown of Delfi-PQ [5].

4.5 Cost Drivers and Mitigations

Based on our ledger and build reviews, the primary hardware cost drivers were:

- **Radio and power electronics:** high share of the electronics budget due to RF PA/LNA devices, power stages, and multiple qualification spins.
- **PCB complexity and count:** stacked, small-form-factor boards with tight tolerances increase per-unit fab costs in low volume.
- **Mechanicals tied to RF:** antennas, precision hardware, and finishing (e.g., plating) are disproportionately expensive in small lots.
- **Spares for education:** deliberate over-procurement to support coursework and remote labs added modest, but intentional, overhead.

Mitigations that proved effective included strict connector/pinout standardization, consolidated BOMs to leverage repeat buys across subsystems, and early procurement of long-lead items (e.g., solar cells) to decouple supply risk from critical design gates.

4.6 Replication Benchmark (Like-for-Like Build)

For planning a follow-on PocketQube of the same capability, a single flight model plus one engineering model can be realized for ~25 k€ (hardware only) under the 2020 pricing basis. Applying observed semiconductor price movements to 2023 and including 21% VAT, the like-for-like procurement estimate is ~27 k€.¹

¹This benchmark assumes the same architecture, batch size, and supply chain; it excludes personnel, facilities, and any new qualification effort.

Key Takeaways for Budgeting. (i) Plan for electronics + PCB to be ~60–65% of hardware cost in low-volume academic builds; (ii) reserve ~25–30% for mechanicals (including RF-critical hardware); (iii) hold an 8–10% line item for test fixtures and generic lab hardware; and (iv) expect 2–4 spins per subsystem to land a flight-ready design without schedule risk.

5. Future Work

The Delfi-Twin mission represents the next step in Delft University of Technology's long-running Delfi program, building on the Delfi-PQ heritage. The mission involves two very small satellites, each about $5 \times 5 \times 17$ cm, designed to fly in formation using differential drag as their only means of control [16, 17]. They will first be launched in a docked configuration to minimize dispersions from rideshare deployment and to allow commissioning with a stable baseline for evaluating GNSS receiver performance (Figure 32). After separation, a small spring-induced Δv of approximately 10 cm/s will create an along-track formation, which can be controlled by varying deployable appendages that modify the satellites' drag area. This enables repeated formation-keeping maneuvers and even collision-avoidance demonstrations, while extending operational lifetime compared to thruster-based systems.

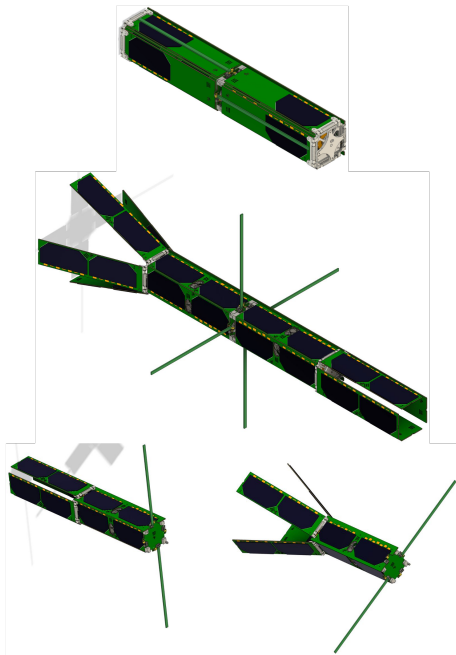


Fig. 32: Delfi Twin Mission, concept of operation.

Equipped with dual-frequency GNSS receivers, the

Delfi-Twins will not only perform in-space precise orbit determination but also provide valuable atmospheric density measurements and drag coefficient calibration. Their operations aim to address upcoming space debris mitigation regulations by demonstrating the feasibility of autonomous traffic management, including timely dissemination of accurate ephemerides to ground operators. By combining space-based GNSS data with ground-based radar, laser, and optical tracking, Delfi-Twin will provide a real-world benchmark for current Space Situational Awareness capabilities [16, 17].

6. Conclusions

Delfi-PQ demonstrates that a 3P PocketQube can deliver credible on-orbit performance using a lean, modular architecture and an academic development model. Over ~two years on orbit (January 13, 2022 to January 6, 2024), the spacecraft sustained routine operations and downlinked more than 40,000 telemetry frames through the Delft ground station and the global amateur community, enabling continuous health assessment and post-flight analysis.

Three results stand out. First, the standardized subsystem core measurably reduced nonrecurring engineering: common MCU, protection, power, and telemetry blocks were replicated across boards, shortening debug cycles and enabling inflight software updates with safe rollback. Second, a COTS-based protection strategy (series limiters plus retriggerable breakers) effectively mitigated single-event latch-ups; on-orbit data show multiple autonomous trip-and-recover events without lasting degradation. Third, the mission highlighted thermo-power coupling as the dominant operational constraint for picoclass platforms: low battery temperatures limited peak current during winter passes, interacting with radio transmit loads and battery protection thresholds. This points to concrete design updates for future missions (e.g., improved charge-path topology, tighter derating of TX duty cycles, and either localized heating or a chemistry more tolerant to low temperatures).

From a cost perspective, hardware development; including multiple design spins and engineering builds, totaled ~86.6 k€ across 2017–2020, with electronics + PCBs accounting for ~64% and mechanicals for ~27%. The same architecture can be reproduced for ~25–27 k€ hardware procurement per flight+engineering pair under recent pricing, validating the affordability of a modular, batch-of-five strategy within university constraints.

In summary, Delfi-PQ validates a repeatable approach for very small spacecraft: enforce modularity through a shared core, prefer simple interfaces and singlestring sys-

tems, protect aggressively against radiation and startup transients, and close the loop between design and operations through rapid iteration. These practices, together with community participation in operations, can extend mission lifetime and deliver research-quality data at low cost—an encouraging baseline for formation-flying successors such as Delfi-Twin.

Acknowledgements

The Delfi-PQ mission was supported by the Delft University of Technology and the Delft Space Institute. Tens of students also contributed to the project as part of their curricular activities and their final graduation projects, and the authors acknowledge their fundamental contributions.

References

- [1] Yue Song, Devi Gnyawali, and Lihong Qian. From early curiosity to space wide web: The emergence of the small satellite innovation ecosystem. *Research Policy*, 53(2):104932, 2024.
- [2] Silvana Radu, Sevket Uludag, Stefano Speretta, Jasper Bouwmeester, Eberhard Gill, and Nikitas Chronas Foteinakis. Delfi-PQ: The first PocketQube of Delft University of Technology. In *Proceedings of 69th International Astronautical Congress*, 2018.
- [3] Jasper Bouwmeester, E. Gill, S. Speretta, and S. Uludag. A new approach on the physical architecture of cubesats & pocketqubes. In *Proceedings of the 15th Reinventing Space Conference*, Glasgow, UK, 2017.
- [4] S. Radu, M.S. Uludag, S. Speretta, J. Bouwmeester, A. Menicucci, A. Cervone, A. Dunn, T. Walkinshaw, P.L. Kaled Da Cas, C. Cappelletti, and F. Graziani. PocketQube Mechanical Interface Standard, 2018.
- [5] M.S. Uludag and S. Speretta. Understanding low-cost satellite development: The delfi-pq case study. In *Proceedings of the Nanosatellite Symposium, Stellenbosch (South Africa), November 25th-27th 2024*, 2024.
- [6] J. Bouwmeester, S.P. van der Linden, A. Povalac, and E.K.A. Gill. Towards an innovative electrical interface standard for pocketqubes and cubesats. *Advances in Space Research*, 62(12):3423–3437, 2018. Advances in Technologies, Missions and Applications of Small Satellites.
- [7] J. Hamann R. J. Bouwmeester, and F. Brouwer G. Delfi-c3 preliminary mission results. In *AIAA Small Satellites Conference 2009*, pages 1–11. American Institute of Aeronautics and Astronautics (AIAA), 2009.
- [8] Jian Guo, Jasper Bouwmeester, and A. Gill E. K. In-orbit results of delfi-n3xt: Lessons learned and move forward. *Acta Astronautica*, 121(April–May):39–50, 2016.
- [9] Silvana Radu, M.S. Uludag, Stefano Speretta, Jasper Bouwmeester, and Andrea Menicucci. Pq9 and cs14 electrical and mechanical subsystem interface standard for pocketqubes and cubesats, 2024. Accessed September 20, 2024.
- [10] Stefano Speretta, Tatiana Pérez Soriano, Jasper Bouwmeester, Johan Carvajal Godínez, Alessandra Menicucci, Trevor Watts, Prem Sundaramoorthy, Jian Guo, and Eberhard Gill. Cubesats to pocketqubes: Opportunities and challenges. In *Proceedings of the 67th International Astronautical Congress (IAC)*. IAF, 2016. 67th International Astronautical Congress, 67th IAC ; Conference date: 26-09-2016 Through 30-09-2016.
- [11] M.S. Uludag, S. Speretta, A. Menicucci, M. van den Bos, C.H. Broekhuizen, M. Biolders, J. Haenen, and E. Gill. A pico-satellite design to demonstrate trajectory and science applications. In *Poster at Small Satellite Conference*, Salt Lake City, Utah, USA, 2020.
- [12] S. Uludag, S. Speretta, E. Gill, J. Bouwmeester, and T.P. Soriano. A new electrical power system architecture for delfi-pq. In *4th IAA Conference on University Satellite Missions and Cubesat Workshop*, pages 511–522. Univelt Inc., 2017.
- [13] S. Uludag M. E. Yakut, S. Speretta, S. Radu, N. Chronas-Foteinakis, J. Bouwmeester, A. Menicucci, and A. Gill E. K. Getting the delfi-pq ready for multiple launch options. In *Proceedings of the International Symposium on Space Technology and Science (Fukui, Japan, June 15–21, 2019)*, 2019. Article 2019-f-08.
- [14] S. Speretta, S. Uludag, V. Karunanithi, S. Radu, N. Chronas Foteinakis, J. Bouwmeester, A. Menicucci, and E. Gill. A multi frequency deployable antenna system for delfi-pq. In *Proceedings of the International Symposium on Space Technology and Science*, Fukui, Japan, 2019.
- [15] M.S. Uludag, S. Speretta, A. Menicucci, and E. Gill. Journey of a pocketqube-concept to orbit. In *Pro-*

ceedings of the International Symposium on Space Technology and Science, Kurume, Japan, 2023.

- [16] Marianna Centrella, Stefano Speretta, Mehmet Şevket Uludağ, and Fabrizio Stesina. Advancing in-space precise tracking: A formation-flying picosatellites mission. In *Proceedings of the 75th International Astronautical Congress (IAC)*, Milan, Italy, October 2024. Paper No. IAC-24-B4.6B.12, Session B4/6B, 14–18 October 2024.
- [17] S. Speretta, R. K. van der Zwaard, and M. S. Uludag. Autonomous formation flying in the traffic. In *Proceedings of Small Satellites for Earth Observation*, pages 1–8, Berlin, Germany, 2025. Article DLR-IAA2025-137.